Probability density optical tomography of confined quasiparticles in a semiconductor microcavity

Gaël Nardin,[a] Taofiq K. Paraïso, Roland Cerna, Barbara Pietka, Yoan Léger, Ounsi El Daif,[b] François Morier-Genoud, and Benoît Deveaud-Plédran
Laboratoire d'Optoélectronique Quantique, École Polytechnique Fédérale de Lausanne (EPFL), Station 3, CH-1015 Lausanne, Switzerland

(Received 29 January 2009; accepted 7 April 2009; published online 6 May 2009)

We present the optical tomography of the probability density of quasiparticles, the microcavity polaritons, confined in three dimensions by cylindrical traps. Collecting the photoluminescence emitted by the quasimodes under continuous nonresonant laser excitation, we reconstruct a three-dimensional mapping of the photoluminescence, from which we can extract the spatial distribution of the confined states at any energy. We discuss the impact of the confinement geometry on the wave function patterns and give an intuitive understanding in terms of a light-matter quasiparticle confined in a box. © *2009 American Institute of Physics*. [DOI: 10.1063/1.3126022]

Probing wave functions or probability densities (PDs) of confined carriers in semiconductor nanostructures is a very elegant way of retrieving textbook solutions of quantum confinement. It could also provide key information on the coupling between different nanostructures. To confine electrons and holes in semiconductor materials, traps in the nanometer range must be engineered due to the small de Broglie wavelength of the carriers. This reduced size generally prevents the optical imaging of the PDs of charge carriers. Sophisticated techniques such as insertion of probe layers,[1,2] magnetotransport measurements,[3] or magnetotunneling[4] allowed however to reconstruct the spatial variation of confined carrier PDs in the growth (vertical) direction of a quantum well (QW). Nevertheless, such techniques are dedicated to the study of PDs along a single confinement axis. They cannot be applied in the case of two-dimensional (2D) or three-dimensional (3D) confining potentials. The study of the in-plane (lateral) spatial extension of electronic wave functions is generally restricted to metallic surfaces and films, using scanning tunneling microscopy[5,6] or synchrotron radiation.[7] The only measurement of fully confined carriers PDs has been achieved using near-field scanning optical microscopy and does not provide a significant resolution to access the spatial variation of the PDs inside the traps.[8]

In our work, we take advantage of the coupling between carriers and light in semiconductor microcavities. In the strong coupling regime, the interaction between excitons (Coulomb-correlated electron-hole pairs) and photons gives rise to the formation of quasiparticles called exciton-polaritons, split in two branches, the upper and lower polaritons.[9] Their dispersion, being dominated by the photonic component, gives them an effective mass 10^4 smaller than the free electron mass. Consequently, they can be confined in micrometer-scale traps, above the resolution of optical microscopes. Moreover, as intracavity polaritons are directly coupled to extracavity photons, with energy and momentum conservation,[10] polaritonic states can be directly imaged through optical detection of the photoluminescence (PL) at the surface of the sample.

We previously engineered a GaAs/AlAs microcavity featuring traps for the photonic modes and a single embedded InGaAs quantum well. The traps for the photonic modes consist in quasicircular mesas of 3 μm diameter, which were etched on the cavity spacer to locally enlarge the cavity length, thus providing a cylindrical potential well for the cavity mode. More details about the sample and its fabrication are given in Ref. 11. The strong coupling between the confined photonic modes and the QW exciton gives rise to zero-dimensional (0D) exciton-polaritons.[11,12]

We nonresonantly excite the system, using a Ti:sapphire cw laser focused on the sample. The diameter of the excitation spot is 30 μm. This hot excitation creates electron hole pairs that relax to the confined and delocalized polariton states.[13,14] Then, due to the coupling with extracavity photons, the eigenmodes emit PL, which is collected with a 0.5 numerical aperture microscope objective and imaged on the slit of a spectrometer using a lens with 25 cm focal length, with a diffraction limited spatial resolution. At the output of the spectrometer, a liquid nitrogen cooled charge-coupled device camera records images of the PL with one spectral dimension and one spatial dimension, as it is presented in Fig. 1(a).

Figure 1(a) shows the PL spectrum of the upper and the lower confined polariton modes as well as the unconfined delocalized 2D modes that are still present around the mesa. One can already observe the spatial distribution of the PD $\|\psi(r)\|^2$ of all the eigenstates along one axis. They can be compared with the solutions of the time-independent Schrödinger equation for a particle confined in a cylindrical trap. Squared values of computed wave functions are presented in Fig. 1(b) at the corresponding computed energies, where we have used an effective polariton mass and confinement potential. Spatial variation of the wave functions, energies, and number of confined states are well reproduced for both upper and lower polaritons. The only consequent qualitative discrepancy occurs for the first excited state of both upper and lower confined polaritons. This state appears doubled whereas the model predicts one state only. It will be shown further that this doublet is a degeneracy lift due to the

[a]Electronic mail: gael.nardin@epfl.ch.
[b]Present address: Institut des Nanotechnologies de Lyon (INL), UMR CNRS 5270, Ecole centrale de Lyon, 36 Avenue Guy de Collongue, 69134 Ecully Cedex, France.

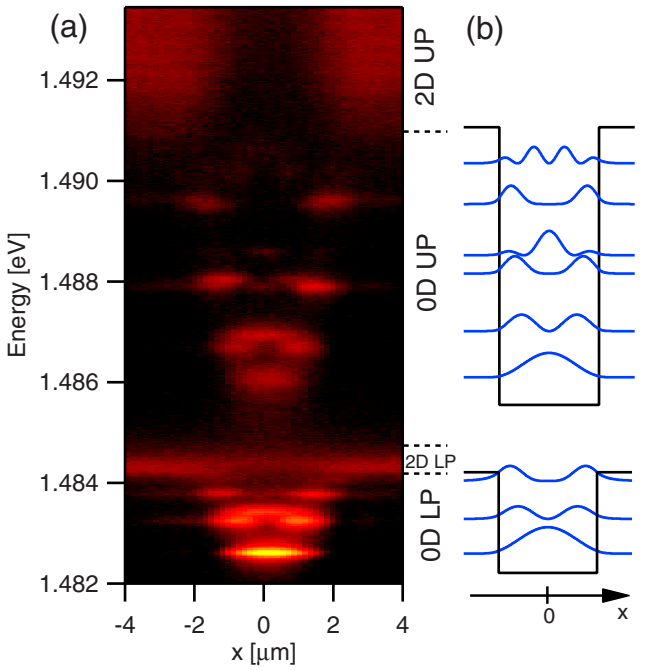

FIG. 1. (Color online) (a) Photoluminescence intensity of a 3 μm polariton mesa as a function of position and energy, in a color log scale. Position $x=0$ corresponds to the center of the mesa. In the margin, dashed lines show the energy ranges in which one can observe the confined lower polariton (0D LP) and upper polariton states (0D UP), and the 2D lower (2D LP) and upper (2D UP) polaritons. The latter is very broad in energy because the large numerical aperture detection integrates over a large angle its photonlike dispersion. (b) Solutions of the time-independent Schrödinger equation for a particle confined in a cylindrical trap. Different effective mass and potential barriers have been used for upper and lower polaritons.

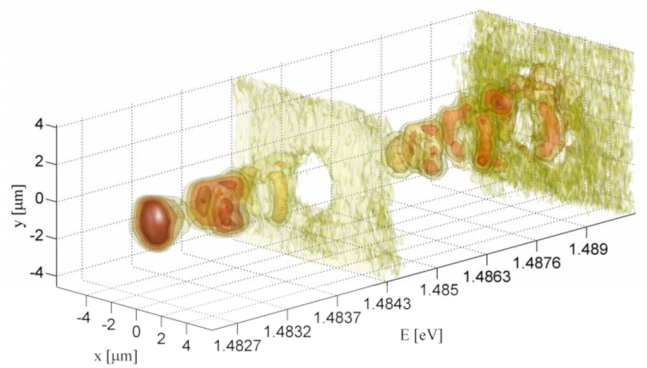

FIG. 2. (Color online) (x, y, E) view of the photoluminescence intensity of the system, constructed by stacking 21 (x, E) intensity plots. Isosurfaces of same intensity are plotted, allowing to map the 2D spatial PD distribution of every confined and extended state for the upper and lower polaritons at the same time. For the sake of visibility, the energy scale is stretched on the lower polariton energy range. To observe easily all confined states PDs, the PL intensity at every energy was multiplied by a Boltzmann factor with $T=30$ *K*, in order to compensate for the quasithermal intensity distribution.

slightly elliptical shape of the confinement potential. Let us note that we do not demonstrate here the quantum nature of the system. Indeed, it was previously shown that the emission spectrum could be very well reproduced classically by first solving Maxwell's equations for the confined photonic modes and then coupling them to the excitonic wave.[12] Nonetheless, a good qualitative agreement is obtained here when using the quasiparticle-in-a-box picture. In our opinion, this model gives a more intuitive understanding of the system than the semiclassical one. This treatment is justified as the photonic confinement, once expressed in the polariton basis, does provide an effective confinement for both upper and lower polaritons, plus a renormalization term of the coupling strength.

We label the confined modes with quantum numbers n and m,[15] $n=1,2,3,\ldots$ giving the number of lobes along the radial direction, $|2m|$ (with $m=0,\pm1,\pm2,\ldots$) giving the number of nodes along the azimuthal direction. The changes of emission intensity between the different confined states in Fig. 1(a) are due to the different photonic fraction of the confined states[16] and to thermalization toward the lower energy states.[13]

In order to perform a full tomography of the system, i.e., to obtain a 2D mapping of the PL at all energies in the same set of data, we scanned the collected PL across the slit of the spectrometer, thus providing the second spatial dimension. We obtain in this way a four-dimensional set of data (x, y, energy, PL intensity), which is presented in a 3D contour plot in Fig. 2, with the PL intensity as a color scale. For the sake of visibility of all the confined states, we corrected the PL intensity at every energy by a Boltzmann factor, in order to counterbalance the thermalization toward the lower energy states. The temperature of the system can be extracted from the PL data as described in Ref. 13. It varies according to the excitation conditions and to the detuning of the photonic modes with respect to the excitonic resonance. All confined states of the upper and lower polaritons are visible, as well as the extended 2D polaritons, at a glance. One can clearly observe here that the luminescence of the 2D polaritons vanishes at the exact position of the mesa. This feature is particularly meaningful for the lower 2D polariton, as it is nearly 100% excitonic at this position. It is a straightforward experimental demonstration that although the confinement is initially acting on the photonic modes only, the excitonic component (and *a fortiori* the entire polariton) is eventually confined as well, due to the strong coupling between the light and the matter wave. This fact comforts us in our description of the polariton as a quasiparticle.

By cutting slices in the (x,y) plane of this set of data we can retrieve 2D mappings of the probability distribution $\|\psi(r,\theta)\|^2$ of any eigenstate, as it is shown in Fig. 3 for the ground state and first two excited states of both the lower [Figs. 3(a)–3(d)] and upper [Figs. 3(e)–3(h)] polaritons. The left column of Fig. 3 shows a ground confined state pattern, with quantum numbers $(n=1,m=0)$, as expected. Let us consider now the first excited state, exhibited on the two central columns of Fig. 3. We must point out that, in principle, in a system with a perfect cylindrical symmetry, $\pm m$ states are degenerate with no fixed phase relation between each other. In time integrated measurement of PL intensity of the eigenstates, this symmetry prevents one from observing any azimuthal variation of the wave function. This is obviously not the case for the first excited state shown in Figs. 3(b), 3(c), 3(f), and 3(g) where one can observe a $(n=1,m=1)$ state pattern featuring two lobes, aligned along two orthogonal axes. This is an unambiguous sign of symmetry breaking already observed spectrally in Ref. 11 due to a slightly elliptical shape of the mesa. This gives rise to a lift of the degeneracy for the $m=\pm1$ states.[17] The two split states then exhibit lobes which are pinned along the main axes of the elliptical confinement potential. This degeneracy lift

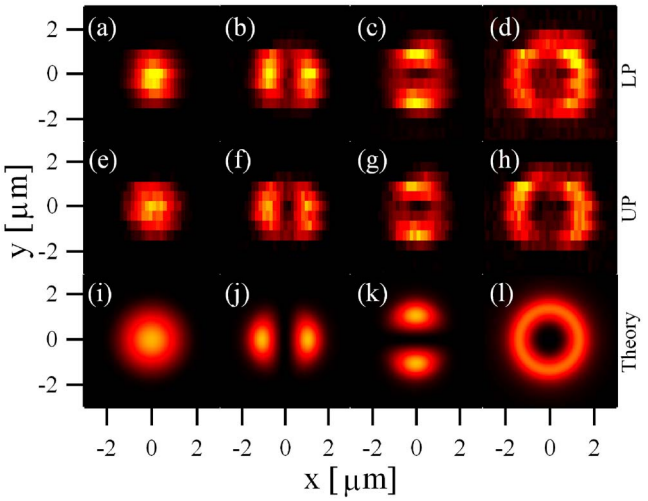

FIG. 3. (Color online) Measured probability density patterns for lower polariton states [(a)–(d)], upper polariton states [(e)–(h)] and solutions of the Schrödinger equation [(i)–(l)], in a linear color scale. Parts (a), (e), and (i) shows a $(n=1,m=0)$ state pattern. Parts (b), (c), (f), (g), (j), and (k) show two quasidegenerate $(n=1,m=1)$ state patterns, the symmetry breaking being due to the elliptical shape of the mesa. Parts (d), (h), and (l) show a $(n=1,m=2)$ state pattern for which the cylindrical symmetry is conserved, the symmetry breaking affecting only $m=\pm 1$ states.

only affects $m=\pm 1$ states because the perturbation on the confinement potential scales as $\cos(2\phi)$, where ϕ is the azimuthal angle. Indeed, for the $(n=1,m=2)$ states displayed in Figs. 3(d) and 3(h), we do not observe lobes, neither a doublet structure.

Figures 3(i)–3(l) show the corresponding solutions of the time-independent Schrödinger equation for a cylindrical confinement. Calculated patterns are similar for both upper and lower polaritons, as changing effective mass and confinement potential mainly changes eigenenergies.[15] Excellent agreement can be observed with measured patterns. An azimuthal variation of the form $e^{im\phi}$ has been applied to Figs. 3(j) and 3(k) in order to reproduce the effect of the symmetry breaking.

In conclusion, we have performed a full (x, y, energy) tomography of the PL of all the confined and unconfined polariton eigenmodes which allows to retrieve 2D spatial probability density mappings for every eigenstate. In particular, these mappings have evidenced the effect of the elliptical geometry of the traps through the breaking of the cylindrical symmetry on the azimuthal PD distribution for $m=\pm 1$ states. Very good qualitative agreement with the solutions of the Schrödinger equation for a cylindrical confinement allows us to give an intuitive interpretation in terms of a quasiparticle confined in a box. This agreement, together with the splitting observed between upper and lower polariton states and the effective confinement observed on both excitonic and photonic components, prove that we have not probed bare optical modes, but the eigenstates of quasiparticles which have a matterwave component. This unique feature leads to very interesting nonlinear responses,[18–20] which allow to imagine applications in the field of nonclassical light emission, such as intricated photon pair emission[20] or single photon emitter,[21] for which a full representation of the spatial extension and linewidth of all the eigenstates, as it was presented in this work, is of crucial importance.

We would like to thank V. Savona, D. Sarchi, K. G. Lagoudakis, M. Wouters, and M. A. Dupertuis for fruitful discussions, and M. Richard and A. Baas for carefully reading the manuscript. We acknowledge support by the Swiss National Research Foundation through the NCCR Quantum Photonics.

[1] J.-Y. Marzin and J.-M. Gérard, Phys. Rev. Lett. **62**, 2172 (1989).
[2] G. Prechtl, W. Heiss, A. Bonanni, W. Jantsch, S. Mackowski, E. Janik, and G. Karczewski, Phys. Rev. B **61**, 15617 (2000).
[3] G. Salis, B. Graf, K. Ensslin, K. Campman, K. Maranowski, and A. C. Gossard, Phys. Rev. Lett. **79**, 5106 (1997).
[4] P. H. Beton, J. Wang, N. Mori, L. Eaves, P. C. Main, T. J. Foster, and M. Henini, Phys. Rev. Lett. **75**, 1996 (1995).
[5] M. F. Crommie, C. P. Lutz, and D. M. Eigler, Science **262**, 218 (1993).
[6] L. Bürgi, O. Jeandupeux, A. Hirstein, H. Brune, and K. Kern, Phys. Rev. Lett. **81**, 5370 (1998).
[7] R. K. Kawakami, E. Rotenberg, H. J. Choi, E. J. Escorcia-Aparicio, M. O. Bowen, J. H. Wolfe, E. Arenholz, Z. D. Zhang, N. V. Smith, and Z. Q. Qiu, Nature (London) **398**, 132 (1999).
[8] K. Matsuda, T. Saiki, S. Nomura, M. Mihara, Y. Aoyagi, S. Nair, and T. Takagahara, Phys. Rev. Lett. **91**, 177401 (2003).
[9] C. Weisbuch, M. Nishioka, A. Ishikawa, and Y. Arakawa, Phys. Rev. Lett. **69**, 3314 (1992).
[10] V. Savona, C. Piermarocchi, A. Quattropani, P. Schwendimann, and F. Tassone, Phase Transitions **68**, 169 (1999).
[11] O. El Daïf, A. Baas, T. Guillet, J.-P. Brantut, R. Idrissi Kaitouni, J. L. Staehli, F. Morier-Genoud, and B. Deveaud, Appl. Phys. Lett. **88**, 061105 (2006).
[12] R. I. Kaitouni, O. El Daif, A. Baas, M. Richard, T. Paraiso, P. Lugan, T. Guillet, F. Morier-Genoud, J. D. Ganière, J. L. Staehli, V. Savona, and B. Deveaud, Phys. Rev. B **74**, 155311 (2006).
[13] T. K. Paraïso, D. Sarchi, G. Nardin, O. El Daif, R. Cerna, Y. Léger, B. Pietka, F. Morier-Genoud, V. Savona, and B. Deveaud-Plédran, Phys. Rev. B **79**, 045319 (2009).
[14] F. Tassone, C. Piermarocchi, V. Savona, A. Quattropani, and P. Schwendimann, Phys. Rev. B **56**, 7554 (1997).
[15] X. Leyronas and M. Combescot, Solid State Commun. **119**, 631 (2001).
[16] The photonic and excitonic fractions are related to the detuning of the photonic mode with respect to the exciton energy.
[17] R. Cerna, D. Sarchi, T. K. Paraïso, G. Nardin, Y. Léger, M. Richard, B. Pietka, O. El Daif, F. Morier-Genoud, V. Savona, M. T. Portella-Oberli, and B. Deveaud-Plédran, arXiv:0904.4444v1.
[18] O. El Daif, G. Nardin, T. K. Paraïso, A. Baas, M. Richard, J.-P. Brantut, T. Guillet, F. Morier-Genoud, and B. Deveaud-Plédran, Appl. Phys. Lett. **92**, 081910 (2008).
[19] G. Nardin, O. El Daif, T. K. Paraïso, A. Baas, M. Richard, F. Morier-Genoud, and B. Deveaud, Phys. Status Solidi C **5**, 2437 (2008).
[20] S. Portolan, P. Hauke, and V. Savona, Phys. Status Solidi B **245**, 1089 (2008).
[21] B. Deveaud-Plédran, C. Ciuti and F. Morier-Genoud, European Patent No. 1729383-A1 (6 December 2006).